Int. J. Multiphase Flow Vol. 15, No. 3, pp. 327—339, 1989
Printed in Great Britain

0301-9322/89 $3.00 + 0.00
Pergamon Press/Elsevier

THE EFFECT OF GAS PROPERTIES ON DROPS IN ANNULAR FLOW

D. M. JEPSON,[1] B. J. AZZOPARDI[2] and P. B. WHALLEY[1]

[1]Department of Engineering Science, University of Oxford, Parks Road, Oxford, England

[2]Thermal Hydraulics Division, Harwell Laboratory, Oxfordshire OX11 0RA, England

(*Received* 1 *October* 1988; *in revised form* 15 *November* 1988)

Abstract—The effect of gas density on the mean drop size and fraction of entrainment in annular two-phase flow has been studied. The data was obtained for a vertical tube of 10.26 mm dia held at a pressure of 1.5 b and ambient temperature. Drop sizes were measured using a laser diffraction technique. Reductions in the gas density show decreases in the entrained liquid fraction whilst the effect on drop size is less certain. This may be obscured by the different entrainment mechanisms, predominating in each fluid system: bag breakup in the helium/water experiments and ligament breakup in the air/water tests. A decrease in the gas density causes the deposition coefficient to increase. The results show that preferential deposition of drops, subsequent to film removal, takes place. At low gas velocities larger drops deposit first by a direct impaction mechanism, whilst at higher velocities small drops deposit out preferentially by diffusion.

Key Words: annular flow, vertical, gas/liquid, drop size, deposition, gas properties

1. INTRODUCTION

Many process industries today employ a wide variety of heat transfer equipment in which gas/liquid flow occurs. One of the more common flow patterns encountered in upward gas/liquid flow is that of annular flow. This is characterized by a central core of fast flowing gas with a slower moving liquid film adjacent to the pipe wall. Beyond critical gas and liquid superficial velocities, the interface becomes highly agitated and "disturbance waves" appear. These waves are torn from the surface giving rise to drop entrainment in the gas core. The liquid film is maintained by drop deposition.

In heat flux controlled systems, such as nuclear reactor cooling systems, depletion of the liquid film occurs by evaporation, as well as entrainment. If the deposition rate, of drops to the film, is smaller than the combined effect of evaporation and entrainment a condition known as dryout is approached, where the liquid film disappears. This brings about a deterioration in the heat transfer coefficient which can lead to large increases in wall temperature, a potentially hazardous condition.

The occurrence of dryout may be predicted from a mass balance on the liquid film, this takes the form

$$\frac{d\dot{m}_{LF}}{dz} = \frac{4}{d_t}\left(D - E - \frac{\theta}{\lambda}\right), \qquad [1]$$

where $\dot{m}_{LF}$ is the film mass flux (flowrate per unit cross-sectional area of tube), z is the distance along the tube, d_t is the tube diameter, D and E are the rates of deposition and entrainment per unit area of tube wall and θ and λ are the heat flux and latent heat, respectively.

Expressions for E have been developed by Hutchinson & Whalley (1973) and Govan *et al.* (1988), whilst deposition, D, thought to be a mass transfer process similar to diffusion, can be defined as follows:

$$D = k_D(c - c_B), \qquad [2]$$

where k_D is a mass transfer coefficient, c is the droplet concentration in the gas and c_B is the wall droplet concentration. Assuming all depositing drops are perfectly absorbed by the liquid film, c_B can be taken as zero. Expressions describing k_D have been generated by Whalley *et al.* (1974), McCoy & Hanratty (1977) and Govan *et al.* (1988).

Advances in the study of droplet deposition by James *et al.* (1980) and Andreussi & Azzopardi (1983), suggest that the previous "diffusional" description of deposition is an oversimplification of the actual process. They believe the deposition process is governed by the drop size/momentum.

Two transport mechanisms have been identified. Small, low, momentum drop, affected by gas-phase eddies, are seen to exhibit fairly random trajectories, analogous with a diffusional-type transport. Whilst larger drops move transversely across the tube in straight lines. This motion, dubbed direct impaction, has been attributed to the atomization process which imparts sufficient momentum to the drops for them to be unaffected by the gas turbulence.

Andreussi & Azzopardi (1983) reanalysed the deposition data of Cousins & Hewitt (1968) and plotted this as $\dot{M}^{+}_{LE}$ against the deposition length on semi-log paper, where $\dot{M}^{+}_{LE}$ defines the dimensionless entrained liquid flowrate, $\dot{M}_{LE1}/\dot{M}_{LE2}$. They postulate that, for drops moving in a diffusion-like manner, measurements of $\dot{M}^{+}_{LE}$ will fall on a straight line, upward deviations from this line indicate an increase in the mass transfer coefficient, and mark the transition to the impaction mechanism of deposition. Consequently, the fraction of drops depositing by direct impaction and by diffusion may be evaluated.

The present investigation is part of a study which continues the work of Willetts (1987) who measured pressured gradients, liquid film flowrates and void fractions in a vertical tube of 10.26 mm dia for a variety of fluid systems: air/water, helium/wate, air/aqueous sulpholane, air/1, 1, 1 trichloroethane and air/fluoroheptane. These fluids allowed the density ratio and surface tension to be varied systematically. The current work extends the above study to include the measurement of drop sizes and deposition.

Here we examine the effect of gas density (using air/water and helium/water systems) on drop size and deposition and use the results to validate the assumptions, made by Andreussi & Azzopardi (1983), concerning droplet deposition.

2. EXPERIMENTAL ARRANGEMENT

2.1. Flow apparatus

Experiments were carried out on the double closed loop rig shown schematically in figure 1, in which both phases were recirculated through a vertical stainless steel test section (i.d. 10.26 mm).

Gas from a multilobe compressor was metered by an orifice plate and fed to the base of the test section. It then passed through a 0.5 m calming section before combining with the liquid.

The liquid was pumped from a stock tank, metered using calibrated rotameters and introduced to the test section through a porous wall section, 0.076 m long. The two-phase flow was allowed to develop over a 3 m length ($\sim$295 dia) after which measurements of film flowrate and droplet size were made.

Downstream of the measurement stations the two-phase mixture was separated. The liquid being returned to the stock tank, whilst the gas was returned, via a buffer vessel, to the compressor inlet.

2.2. Film flowrate and deposition measurements

The liquid film flowrate was determined by withdrawing a portion of the flow through a porous wall section, separating the phases and measuring the rate of liquid collection. In all cases the quantity of gas removed was kept below 5% of the total gas flow. This was found to have no effect on the measured values of film flowrate and drop size.

Because entrainment and deposition occur simultaneously they are difficult to measure. Removal of the liquid film will suppress entrainment and allow the study of droplet deposition. The subsequent build up of a new liquid film over a tube length, was monitored using a second porous wall device.

Assuming homogeneous flow in the gas/liquid core and a liquid density far greater than the gas density, the deposition mass flux, D, appearing in [2] can be written as

$$D = \frac{k_D \dot{M}_{LE} \rho_G}{\dot{M}_G}, \qquad [3]$$

where $\dot{M}_{LE}$ and $\dot{M}_G$ are the entrained liquid and gas flowrates, respectively, and ρ_G is the gas density.

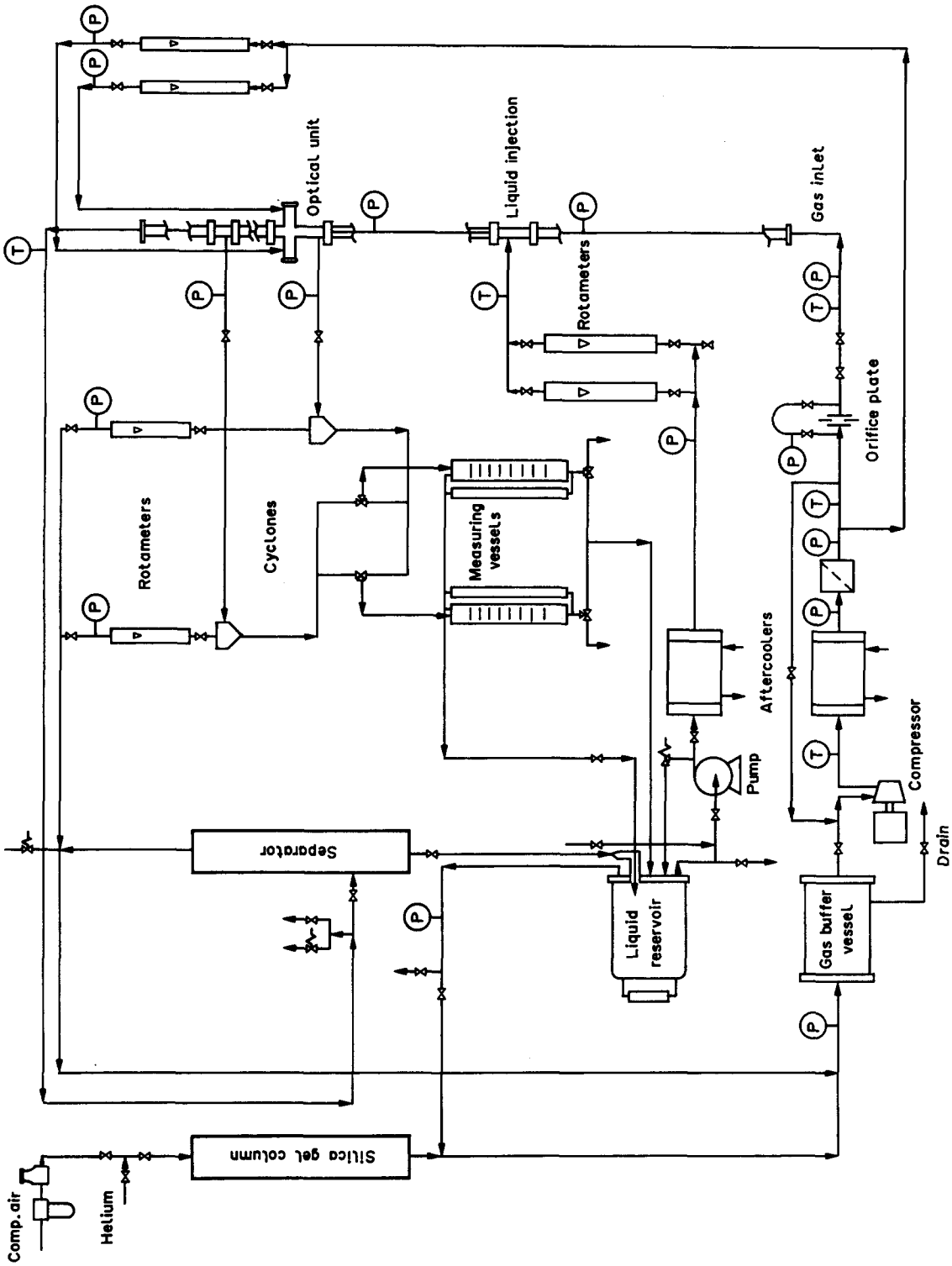

Figure 1. Double closed loop rig.

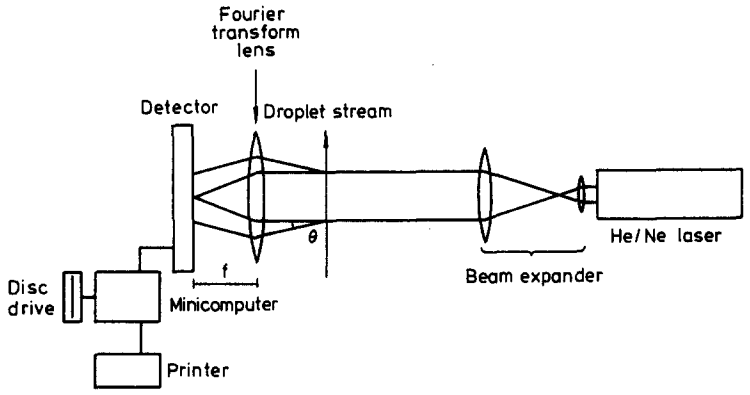

Figure 2. Schematic layout of the Malvern particle sizer.

Performing a mass balance over a small increment of flow length where unidirectional deposition is occurring; and integrating for the conditions pertaining at the first and second liquid film removal points yields a description of the deposition mass transfer coefficient:

$$k_D = \frac{\dot{M}_G}{\pi d_t \rho_G z_D} \ln\left(\frac{\dot{M}_{LE1}}{\dot{M}_{LE2}}\right), \quad [4]$$

where z_D is the deposition length, which was varied between 0.193 and 1.094 m.

2.3. Drop size measurements

Drop sizes were measured using the laser diffraction technique developed by Swithenbank *et al.* (1976) and applied to annular flows by Azzopardi (1985) and Teixeira *et al.* (1987).

This technique is based on the Fraunhofer diffraction of a parallel beam of monochromatic light by moving drops. A sizing instrument, utilizing this technique, is manufactured by Malvern Instruments Ltd. The unit's optical arrangement and instrumentation is shown in figure 2. It comprises a 3 mW He/Ne laser whose beam is expanded to a diameter of approx. 7 mm. The beam is directed at a drop sample, and a Fourier transform lens placed in the light path, after the sample, is used to focus the diffracted and undiffracted light onto a detector which consists of 30 semicircular photosensitive elements. These monitor the angular distribution of the scattered light.

Because each element has associated with it a characteristic drop size range, the light energy distribution, collected by each element, $L(I)$, can be related to the drop size distribution of that element $W(J)$, by the matrix equation

$$L(I) = T(I, J)W(J), \quad [5]$$

where $T(I, J)$ is a square matrix, containing coefficients characteristic of each detector element. Solution of [5] provides the drop size distribution. Rather than solve [5] directly, the system assumes the drop distributed can be modelled by an appropriate distribution function, in this case the Rosin–Rammler distribution, defined below:

$$R = \exp\left[\left(\frac{-d_p}{\bar{X}}\right)^N\right], \quad [6]$$

where R is the volume fraction of drops with diameters greater than d_p, and X and N are the characteristic size and width parameters of the distribution. These parameters are adjusted iteratively to give the best agreement between the calculated and measured values of $L(I)$. The suitability of this equation for describing the drop size distribution in annular flows has been proven from the photographic results of Cousins & Hewitt (1968) and Andreussi *et al.* (1978). The accuracy of the instrument has been checked by Azzopardi (1985) and Teixeira *et al.* (1987).

3. RESULTS

Measurements of droplet size and film flowrates were made on the "double closed loop rig", for the fluid systems air/water and helium/water at ambient temperature. In all experiments, bar those

Table 1. Air/water data

Superficial gas velocity (m/s)	Liquid mass flux (kg/m² s)	Sauter mean diameter, d_{32} (μm)				Entrained liquid mass flux (kg/m² s)				Deposition mass transfer coefficient (m/s)		
		Datum	0.2 m	0.6 m	0.9 m	Datum	0.2 m	0.6 m	0.9 m	0.2 m	0.6 m	0.9 m
22.22	40	173.23	—	—	—	0.472	—	—	—	—	—	—
	60	154.12	—	—	—	0.839	—	—	—	—	—	—
	80	147.97	—	—	—	1.317	—	—	—	—	—	—
	100	—	—	—	—	2.080	—	—	—	—	—	—
	120	140.16	99.73	92.24	—	1.995	—	—	—	—	—	—
	140	126.02	90.74	89.46	—	1.967	—	—	—	—	—	—
33.33	40	67.92	63.08	71.48	74.63	0.813	—	—	—	—	—	—
	60	67.12	63.88	72.09	73.90	2.063	—	—	—	—	—	—
	80	66.23	60.66	64.81	63.54	4.767	2.786	1.981	1.928	0.234	0.126	0.085
	100	67.63	58.81	58.78	56.43	6.892	3.939	2.455	1.939	0.243	0.146	0.119
	120	67.80	58.15	58.04	57.75	8.043	4.216	2.362	1.636	0.281	0.173	0.149
	140	68.63	56.84	57.04	59.26	9.519	4.788	2.212	2.003	0.299	0.206	0.146
44.44	40	43.58	42.87	49.85	53.27	2.666	—	—	—	—	—	—
	60	41.41	42.18	48.95	51.71	6.737	4.458	3.855	3.573	0.240	0.105	0.079
	80	43.12	42.28	47.18	47.24	10.228	6.658	3.503	2.970	0.249	0.202	0.155
	100	42.57	42.37	46.76	48.62	14.510	9.442	5.806	4.263	0.249	0.172	0.153
	120	44.38	42.31	47.82	49.19	17.587	10.835	6.378	4.513	0.281	0.191	0.152
	140	44.32	42.45	48.03	48.94	21.777	13.216	7.927	6.445	0.290	0.190	0.152
55.56	40	32.93	32.38	40.64	44.55	6.274	—	4.441	—	—	0.081	—
	60	31.76	33.42	40.94	44.49	10.949	7.732	5.671	4.593	0.252	0.155	0.136
	80	33.53	35.48	42.04	43.57	18.450	13.453	8.879	6.871	0.229	0.172	0.154
	100	34.66	36.65	43.21	44.10	24.592	17.647	11.871	8.978	0.241	0.171	0.158
	120	35.76	38.39	44.11	44.50	30.846	21.666	14.256	11.536	0.256	0.182	0.154
66.67	40	26.49	27.02	34.67	36.99	7.724	—	5.580	4.238	—	0.092	0.113
	60	26.92	29.58	35.50	37.36	14.745	10.744	7.513	5.050	0.275	0.190	0.201

Table 2. Helium/water data

Superficial gas velocity (m/s)	Liquid mass flux (kg/m² s)	Sauter mean diameter d_{32} (μm)			Entrained liquid mass flux (kg/m² s)			Deposition mass transfer coefficient (m/s)	
		Datum	0.2 m	0.6 m	Datum	0.2 m	0.6 m	0.2 m	0.6 m
44.44	60	85.95	—	—	0.415	—	—	—	—
	80	77.66	63.91	—	1.249	—	—	—	—
	100	72.25	55.79	57.59	3.291	—	—	—	—
	120	71.83	50.92	51.82	3.718	—	1.847	—	0.138
	140	61.67	47.73	48.50	4.840	2.729	2.281	0.348	0.148
	147	56.81	—	—	6.434	—	—	—	—
55.56	40	60.75	44.69	—	0.361	—	—	—	—
	57	48.92	—	—	0.766	—	—	—	—
	60	48.62	38.48	—	0.834	—	—	—	—
	80	37.49	35.55	44.01	2.386	—	0.996	—	0.215
	100	32.85	32.54	38.71	4.103	—	1.935	—	0.185
	120	29.59	28.91	33.83	6.114	3.526	2.553	0.418	0.215
	140	26.74	27.06	31.83	8.414	5.068	3.327	0.385	0.229
66.67	40	32.72	32.49	—	1.032	—	—	—	—
	60	27.60	25.58	—	1.379	—	—	—	—
	80	23.54	22.93	28.31	4.167	2.229	1.416	0.570	0.319
	100	20.90	20.73	26.09	7.190	4.230	2.542	0.483	0.307
	120	19.68	19.93	24.41	11.310	7.219	4.318	0.409	0.284
	140	19.34	19.93	23.75	14.785	9.520	5.462	0.401	0.294
75.56	40	25.00	24.93	—	1.703	—	—	—	—
	57	21.08	—	—	3.469	—	—	—	—
	60	21.66	21.61	—	2.924	—	—	—	—
	80	18.51	19.36	23.50	6.337	3.859	2.320	0.498	0.327
	100	17.51	18.43	22.11	10.397	6.598	3.761	0.456	0.331

duplicating the test conditions of Cousins & Hewitt (1968), a pressure of 1.5 b was maintained at the measuring point. The liquid mass flux was varied in the range 40–140 kg/m² s, whilst the gas superficial velocity was varied between 22–76 m/s.

Measurements were made at, and 0.2, 0.6 and 0.9 m above, the first film removal point. From these measurements, deposition coefficients, k_D, were calculated, using [4].

The air/water and helium/water data are presented in tables 1 and 2, respectively. An example of deposition coefficient information is given in figure 3, where the present results are seen to agree with those of Cousins & Hewitt (1968). The drop size data are shown in figures 4 and 5, where behaviour similar to that observed by Azzopardi (1985) and Teixeira *et al.* (1987) is seen. Here, gas velocity has a marked effect on drop size whilst the effect of liquid flow is far less, being more pronounced at the lower liquid flowrates.

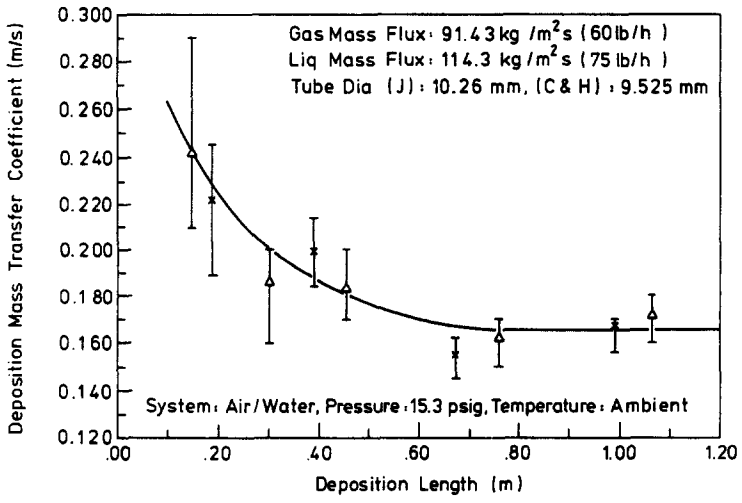

Figure 3. Effect of deposition length on the deposition mass transfer coefficient. A comparison of the current data (×) with that of Cousins & Hewitt (1968) (△).

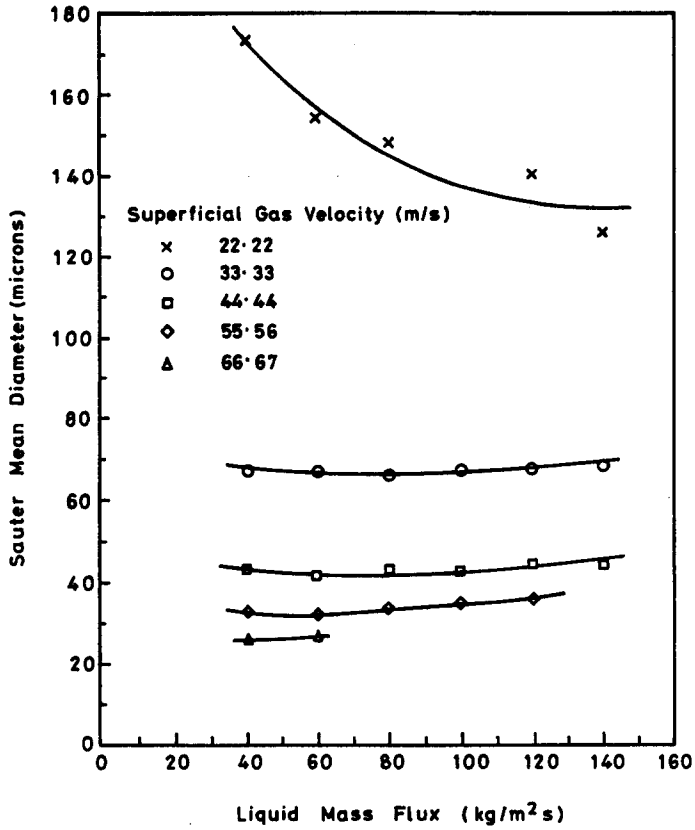

Figure 4. Influence of liquid mass flux on drop size. (System = air/water, pressure = 7.5 psig, temperature = ambient.)

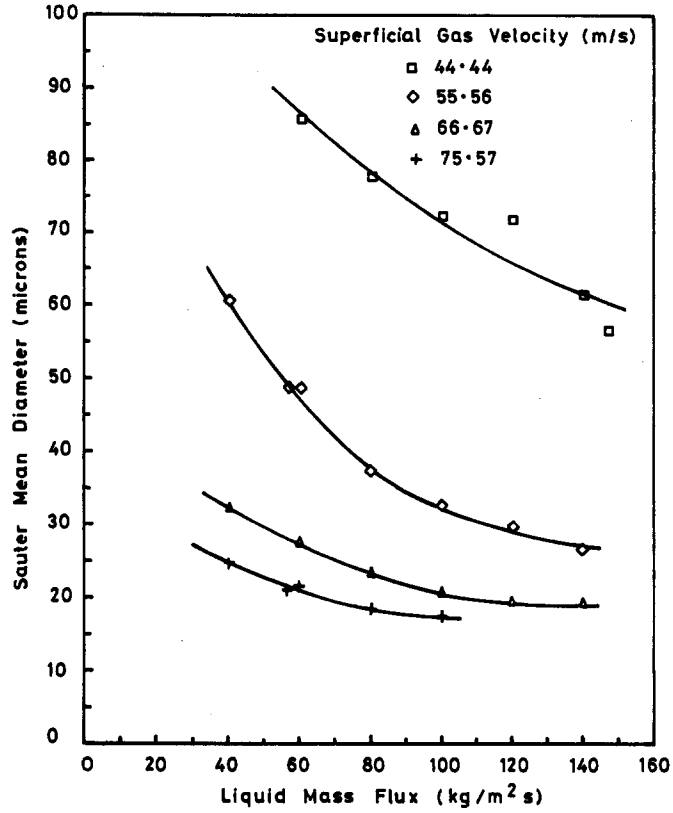

Figure 5. Influence of liquid mass flux on drop size. (System = helium/water, pressure = 7.5 psig, temperature = ambient.)

4. DISCUSSION

4.1. Deposition mass transfer coefficient

The deposition mass transfer coefficient, deduced from experiments where the film was removed and entrainment suppressed, varies with the deposition length, figure 3. Initially the coefficient decreases rapidly with increasing deposition length and then asymptotes to an almost constant value. Similar behavior has been observed by Cousins & Hewitt (1968), who suggest that the rapid fall is related to the change in drop size along the deposition length. They propose that the larger drops deposit first. Because a high percentage of the entrained liquid resides in these drops, the fall in the entrained fraction and hence in the mass transfer coefficient is initially great.

Evidence that this might be the case came to light when James *et al.* (1980) combined the idea of Hutchinson *et al.* (1971), regarding the interaction of "small" drops with gas-phase eddies, and the observations of Whalley *et al.* (1979), on the radial motion of larger drops in tubes. They suggest that the larger drops, with their higher momentum, are insensitive to gas turbulence, and travel laterally across the tube in straight lines to deposit by a mechanism dubbed direct impaction. The smaller drops, with their lower momentum are more susceptible to buffeting by gas-phase eddies and trace fairly random trajectories, prior to their diffusional deposition.

Because the radial distance travelled by the high momentum drops is smaller than that traced by the slow momentum drops, it follows that the larger, high momentum drops will deposit first.

An examination of Cousins & Hewitt's (1968) data by Andreussi & Azzopardi (1983) revealed that the fraction of drops depositing by the diffusional mechanism increased as the superficial gas velocity increased, but was insensitive to pressure. A similar analysis of data taken on the double closed loop rig shows excellent agreement.

Tables 1 and 2 show the deposition coefficients, from the lower density helium/water system, to be slightly higher than those from the air/water experiments. Drop concentrations were lower for the helium/water system but as with the air/water data no noticeable effect of concentration was present.

4.2. Drop sizes

Drop sizes data for the fluid systems air/water and helium/water are listed in tables 1 and 2 and plotted in figures 4 and 5. Both systems show the drop size decreasing with increasing superficial gas velocity. Given that a critical Weber number identifies the maximum stable drop size permissible, where the Weber number, $(\rho_G U_G^2 d_p)/\sigma$, is a balance between the disruptive inertial and stabilizing surface tension forces, increasing the gas velocity will cause a decrease in drop size.

For increasing liquid mass flux the air/water system shows the drop size, in all but the lowest gas velocity case, to decrease first and then increase, whilst the drop size in the helium/water system merely shows a decrease. An apparent difference between the two flows is the lower shear, $(\propto \rho_G U_G^2)$, of the helium, which gives rise to less entrainment. Azzopardi (1985) has identified the dependence of drop size on the entrained liquid flowrate. Plotting both drop size data sets against entrained liquid flow, figure 6, shows that data, where drop size decreases with increasing liquid flow, occupy similar regions.

Two "lines of thought" are presented which may explain the variation in drop size with entrained liquid flow. In one case, it is suggested, that increasing entrainment, at low entrained liquid flowrates, amplifies the gas-phase turbulence, causing a reduction in the drop size. Opposing this mechanism is the process of coalescence. Initially, at low concentrations, coalescence will be insignificant, as the concentration rises coalescence becomes more dominant and the drop size increases.

The second explanation follows from the visualization studies of Azzopardi (1983), where the minimum in the drop size vs liquid flowrate was observed to coincide with the boundary between atomization mechanisms. At low liquid flowrates the gas undercuts the disturbance wave forming a "bag". This bag, comprising a thin skin and thicker rim, breaks giving smaller drops from the skin, and larger drops from the rim. At higher liquid flowrates, the wave crests are torn off in the form of ligaments which are subsequently broken up by the gas stream. It is suggested that the bag breakup mechanism forms larger drops than the ligament breakup mechanism. Assuming both mechanisms occur simultaneously, where the ligament mechanism predominates at higher liquid

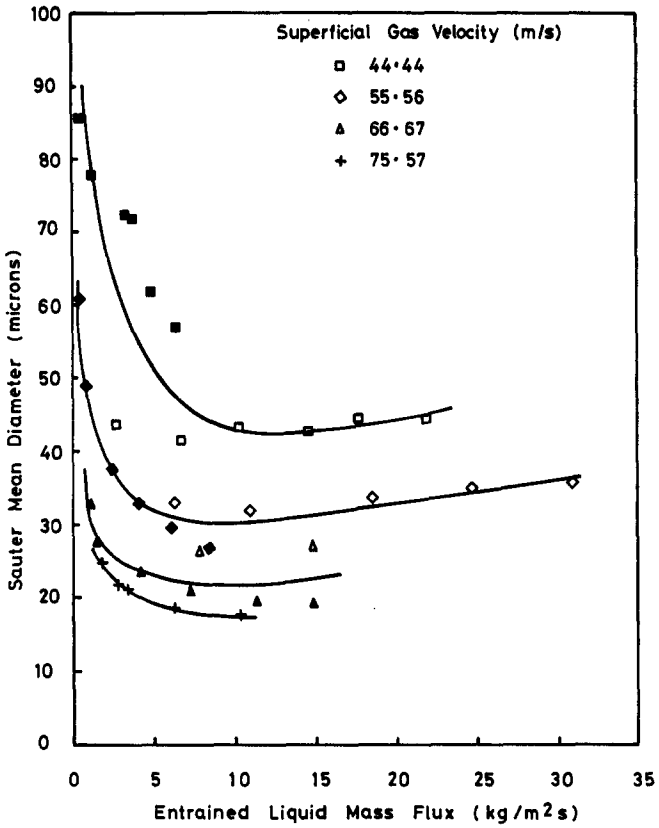

Figure 6. Influence of entrained mass flux on drop size. Open symbols—air/water data; solid symbols—helium/water data. (Pressure = 7.5 psig, temperature = ambient.)

flowrates, then the observed drop size should fall with increasing liquid flowrate. However, as the liquid flowrate increases in the region where ligament breakup predominates, the created drop size will not change, but the observed size should increase because coalescence has occurred.

From the results shown in figure 6, the effect of gas density on drop size can be deduced. For the limited data set where gas velocity and entrained liquid flowrate can be matched for both fluid systems, the drop size varies with gas density to the power of 0.1. This increase in drop size with gas density was also detected by Gibbons (1985), who varied the gas density by altering the experimental pressure, whilst maintaining the gas and liquid flowrates. Gibbons (1985) suggests that drop size depends on gas density to the power of 0.4. Because these experiments were performed maintaining the gas and liquid flowrates, corrections must be applied to allow for the differences in gas velocity and entrained liquid flowrate. This made the data of Gibbons difficult to interpret, so not surprisingly there is qualitative not quantitative agreement between his results and the present data.

A number of equations have been proposed to predict the size of drops, Azzopardi *et al.* (1980) suggests the following equation, which is specific to those flowrates where drop size increases with liquid flowrate; this means it cannot be applied to the helium/water systems:

$$\frac{d_{32}}{d_t} = 1.91 \frac{\mathrm{Re}^{0.1}}{\mathrm{We}^{0.6}} \left(\frac{\rho_G}{\rho_L}\right)^{0.6} + 0.4 \frac{\dot{m}_{LE}}{\rho_L U_G}, \qquad [7]$$

where

$$\mathrm{Re} = \frac{\rho_G U_G d_t}{n_G}$$

and

$$\mathrm{We} = \frac{\rho_G U_G^2 d_t}{\sigma}.$$

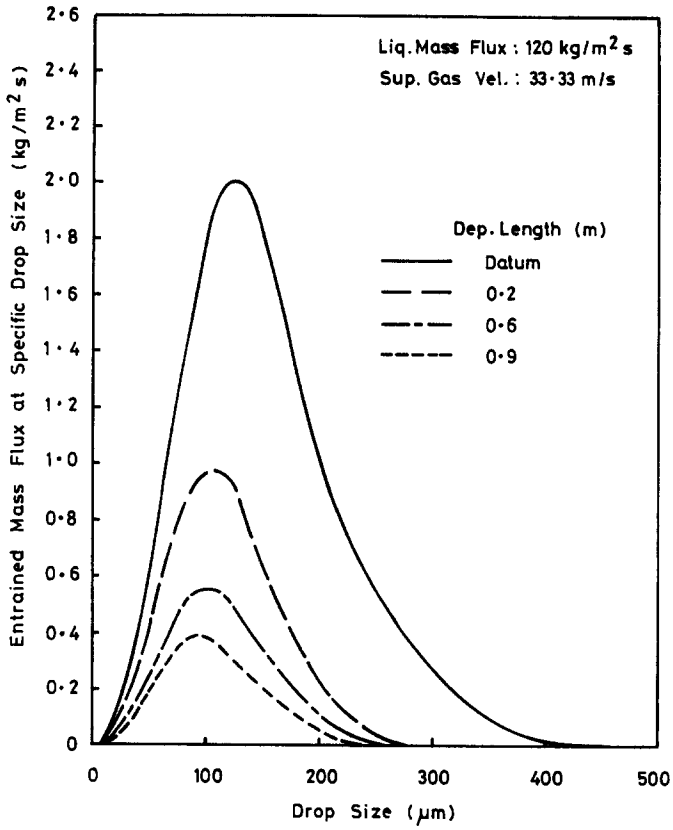

Figure 7. Quantity of the total liquid entrainment at a specific drop size (air/water); $U_G = 33$ m/s, $\dot{m}_L = 120\,kg/m^2\,s$.

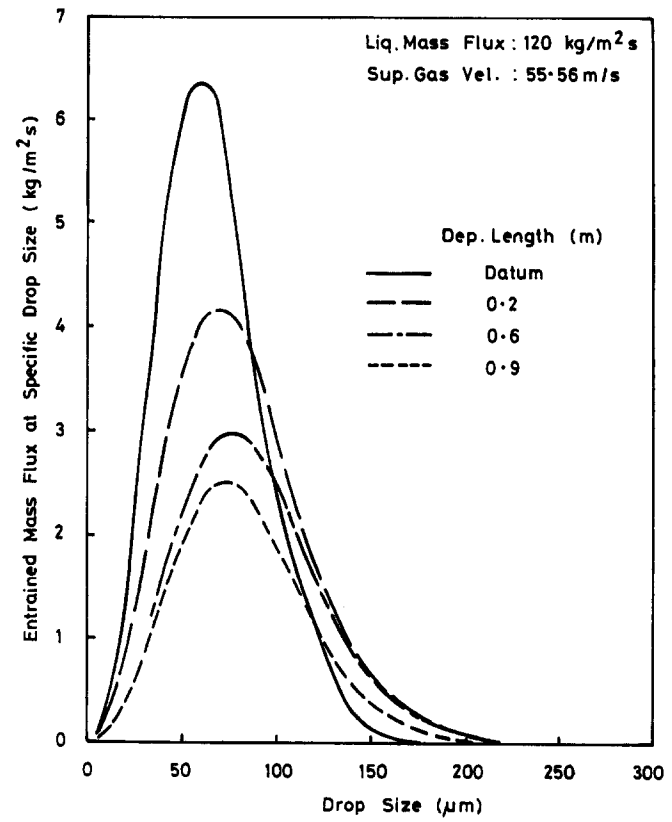

Figure 8. Quantity of the total liquid entrainment at a specific drop size (air/water); $U_G = 56$ m/s, $\dot{m}_L = 120\,kg/m^2\,s$.

This shows a dependence on gas density to the power of 0.1 and on tube diameter of 0.5. Nonetheless, predictions of drop sizes for the air/water system are 30% low.

Subsequently, Azzopardi (1985) proposed an equation omitting the tube diameter term, and once again specific to conditions promoting an increase in drop size:

$$\frac{d_{32}}{\lambda} = \frac{15.4}{\mathrm{We}^{0.58}}\left(\frac{\rho_G}{\rho_L}\right)^{0.58} + 3.5\frac{\dot{m}_{LE}}{\rho_L U_G}, \qquad [8]$$

where

$$\mathrm{We} = \rho_G U_G^2 \lambda/\sigma$$

and

$$\lambda = \sqrt{\frac{\sigma}{\rho_L g}}.$$

This equation, which was based on, and correctly predicts, data from tubes of 0.032 and 0.125 m dia, gives expected drop sizes 50% above those measured in the air/water experiments. Azzopardi acknowledges, that for narrow tubes, a tube diameter effect is expected.

4.3. Effect of deposition on drop size

Drop size data taken at, and 0.2, 0.6 and 0.9 m above, the first film removal point have been examined for evidence of the preferential deposition of specific drop sizes. The data in tables 1 and 2 show that some mean sizes increased whilst others fell and then increased with deposition length.

Bearing in mind the analysis of Andreussi & Azzopardi (1983) we were able to determine, for both fluid systems, the fraction of drops that would deposit by direct impaction. For the air/water

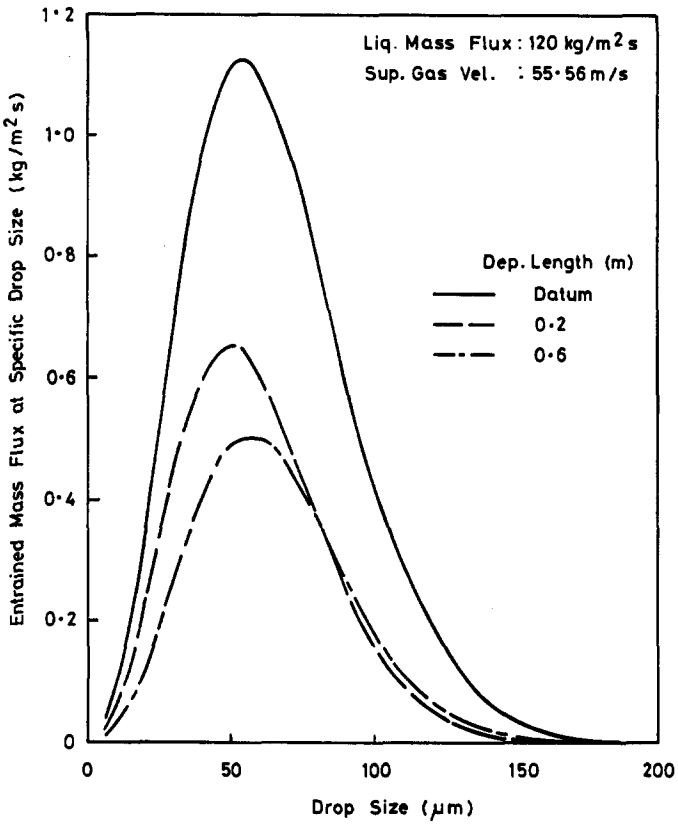

Figure 9. Quantity of the total liquid entrainment at a specific drop size (helium/water); U_G = m/s; $\dot{m}_L = 120\ \mathrm{kg/m^2\,s}$.

system, at a gas velocity of 33 m/s, corresponding to 38% deposition by direct impaction, the larger drops deposit preferentially, figure 7. In contrast, at the higher superficial gas velocity of 56 m/s, where the fraction of drops depositing by direct impaction is only 15%, the smaller drops deposit initially, figure 8. The preferential deposition of these smaller drops is in keeping with the diffusion-like theory, where the smaller the drop the more likely the deposition. In addition the fraction of entrained liquid residing at the larger drop sizes has increased and is probably a result of coalescence between the small fast moving drops and the larger slower moving drops.

These trends are also mirrored by the helium/water data. However for a given superficial gas velocity the fraction of drops which deposit by direction impaction has increased, figure 9. Given the nature of the bag entrainment mechanism, predominating in the helium/water system, this might be expected. It is believed this mechanism produces larger drops than the ligament mechanism, which predominates in the air/water system. The high momentum of these large drops makes them less susceptible to the effect of gas turbulence and more likely to impact deposit.

5. CONCLUSIONS

The following conclusions may be drawn:

(1) A reduction in gas density causes a decrease in the amount of entrainment. This can be explained by the lower shear ($\propto \rho_G U_G^2$) in the helium gas.

(2) Droplet size is seen to decrease with increasing superficial gas velocity. Given that a critical Weber number identifies the maximum stable drop size permissible, where the Weber number, $(\rho_G U_G^2 d_p)/\sigma$, is a balance between the inertial and surface tension forces, increasing the gas velocity causes a decrease in drop size.

(3) For increasing liquid mass flux the air/water system shows that the drop size, in all but one case, decreases first and then increases, whilst the drop size in the helium/water system just shows a decrease. At low drop concentrations, increasing the entrainment may amplify the disruptive gas-phase turbulence, causing the drop size to reduce. At high drop concentrations coalescence becomes the dominant factor, and the drop size rises. Additionally, the observations of Azzopardi (1983) indicate that the minimum seen in drop size vs liquid flowrate marks the transition between entrainment mechanisms: bag breakup predominating at the low liquid flowrates, and ligament breakup occurring at the higher liquid flowrates. He suggests that bag breakup produces larger drops than those seen from the ligament breakup. Assuming both mechanisms occur simultaneously the observed drop size will fall, as the predominating entrainment mechanism shifts from bag to ligament. Drop size will then rise as the increase in drop concentration starts to promote coalescence.

(4) The data show that at low gas velocities larger drops deposit preferentially, whilst at higher gas velocities smaller drops deposit first. This provides confirmation of the suggestions of Andreussi & Azzopardi (1983) that there are two mechanisms of deposition: direct impaction predominating at low velocities with preferential deposition of larger drops, and diffusion-like deposition at higher velocities where smaller drops deposit first.

(5) The deposition coefficients measured in the present work are similar to those of Cousins & Hewitt (1968). The data show a rapid decrease in the mass transfer coefficient with increasing deposition length, this asymptotes to an almost constant value. It is suggested that large drops, which contain a high percentage of the entrained liquid, deposit out first by direct impaction. This causes the change in the entrained liquid flowrate, and hence k_D, to be large. A decrease in gas density causes the deposition coefficient to increase.

Acknowledgements—The work described in this report was undertaken as part of the Underlying Research Programme of the UKAEA. A SERC CASE award is held by D.M.J.

REFERENCES

ANDREUSSI, P. & AZZOPARDI, B. J. 1983 Droplet deposition and interchange in annular gas–liquid flow. *Int. J. Multiphase Flow* **9**, 681–695.

ANDREUSSI, P., ROMANO, G. & ZANELLI, S. 1978 Drop size distribution in annular mist flows. Presented at *1st Int. Conf. on Liquid Atomization and Spray Systems*, Tokyo.

AZZOPARDI, B. J. 1983 Mechanism of entrainment in annular two-phase flow. UKAEA Report AERE-R11068.

AZZOPARDI, B. J. 1985 Drop sizes in annular two-phase flow. *Expts Fluids* **3**, 53–59.

AZZOPARDI, B. J., FREEMAN, G. & KING, D. J. 1980 Drop size and deposition in annular two-phase flow. UKAEA Report AERE-R9634.

COUSINS, L. B. & HEWITT, G. F. (1968) Liquid phase mass transfer in annular two-phase flow: droplet deposition and liquid entrainment. UKAEA Report AERE-R5657.

GIBBONS, D. B. (1985) Drop formation in annular two-phase flow. Ph.D. Thesis, Univ. of Birmingham.

GOVAN, A. H., HEWITT, G. F., OWEN, D. G. & BOTT, T. R. 1988 An improved CHF modelling code. Presented at *2nd U.K. Natn. Heat Transfer Conf.*, Strathclyde Univ., Glasgow.

HUTCHINSON, P. & WHALLEY, P. B. 1973 A possible characterisation of entrainment in annular flow. *Chem. Engng Sci.* **28**, 974–975.

HUTCHINSON, P., HEWITT, G. F. & DUKLER, A. E. 1971 Deposition of liquid or solid dispersions from turbulent gas streams: a stochastic model. *Chem. Engng Sci.* **26**, 419–439.

JAMES, P. W., HEWITT, G. F. & WHALLEY, P. B. 1980 Droplet motion in two-phase flow. UKAEA Report AERE-R9711.

MCCOY, D. D. & HANRATTY, T. J. 1977 Rate of deposition of droplets in annular two-phase flow. *Int. J. Multiphase Flow* **3**, 319–331.

SWITHENBANK, J., BEER, J. M., TAYLOR, D. S., ABBOT, D. & MCCREATH, G. C. 1976 A laser diagnostic for the measurement of droplet and particle size distribution. Report No. AD-A021.130, AFOSR-TR-76.0068, Dept of Chem. Engng and Fuel Technol., Sheffield Univ.

TEIXEIRA, J. C. F., AZZOPARDI, B. J. & BOTT, T. R. 1987 The effect of inserts on drop sizes in vertical annular flow. UKAEA Report AERE-R12641.

WHALLEY, P. B., HUTCHINSON, P. & HEWITT, G. F. 1974 The calculation of critical heat flux in force convection boiling. Presented at *5th Int. Heat Transfer Conf.*, Tokyo, Paper B6.11.

WHALLEY, P. B., HEWITT, G. F. & TERRY, J. W. 1979 Photographic studies of two-phase flow using a parallel light technique. UKAEA Report AERE-R9389.

WILLETTS, I. P. 1987 Non-aqueous annular two-phase flow. D. Phil. Thesis, Univ. of Oxford.